Nonlinear vibration analysis of piezoelectric plates reinforced with carbon nanotubes using DQM

Ali Ghorbanpour Arani[1], Reza Kolahchi[*2] and Masoud Esmailpour[3]

[1]*Faculty of Mechanical Engineering, Institute of Nanoscience & Nanotechnology,*
University of Kashan, Kashan, Iran
[2]*Department of Mechanical Engineering, Kashan Branch,*
Islamic Azad University, Kashan, Iran
[3]*Young Researchers and Elite Club, Damavand Branch,*
Islamic Azad University, Damavand, Iran

Abstract. The aim of the paper is to analyze nonlinear transverse vibration of an embedded piezoelectric plate reinforced with single walled carbon nanotubes (SWCNTs). The system in rested in a Pasternak foundation. The micro-electro-mechanical model is employed to calculate mechanical and electrical properties of nanocomposite. Using nonlinear strain-displacement relations and considering charge equation for coupling between electrical and mechanical fields, the motion equations are derived based on energy method and Hamilton's principle. These equations can't be solved analytically due to their nonlinear terms. Hence, differential quadrature method (DQM) is employed to solve the governing differential equations for the case when all four ends are clamped supported and free electrical boundary condition. The influences of the elastic medium, volume fraction and orientation angle of the SWCNTs reinforcement and aspect ratio are shown on frequency of structure. The results indicate that with increasing volume fraction of SWCNTs, the frequency increases. This study might be useful for the design and smart control of nano/micro devices such as MEMS and NEMS.

Keywords: nonlinear vibration; piezoelectric plate; SWCNT; pasternak foundation; DQM

1. Introduction

Nanocomposites hold the promise of advances that exceed those achieved in recent decades in composite materials. The nanostructure created by a nanophase in polymer matrix represents a radical alternative to the structure of conventional polymer composites. These complex hybrid materials integrate the predominant surfaces of nanoparticles and the polymeric structure into a novel nanostructure, which produces critical fabrication and interface implementations leading to extraordinary properties (Kotsilkova 2007).

Piezoelectricity is a classical discipline traced to the original work of Jacques and Pierre Curie around 1880. This phenomenon describes the relations between mechanical strains on a solid and its resulting electrical behavior resulting from changes in the electric polarization. One can create

---

∗Corresponding author, Dr., E-mail: r.kolahchi@gmail.com

an electrical output from a solid resulting from mechanical strains, or can create a mechanical distortion resulting from the application of an electrical perturbation (Antonio Arnau 2008). Piezoelectric materials have been used to manufacture various sensors, conductors, actuators, etc. in fact, they have become one of the smart materials nowadays (Chen *et al.* 2004).

Regarding research development into the use of nanocomposite, Kireitseu (2007) concentrates on an investigation related to nanoparticle-reinforced materials dynamic characterization and modelling of relationships between structure and mechanical properties of the materials across the length scales. Dynamic stability analysis of functionally graded nanocomposite beams reinforced by SWCNTs based on Timoshenko beam theory was studied by Ke *et al.* (2011). Murmu and Adhikari (2011) analyzed vibration of nonlocal double-nanoplate- system (NDNPS). Their study highlighted that the small-scale effects considerably influence the transverse vibration of NDNPS. Besides, they elucidated that the increase of the stiffness of coupling springs in the NDNPS reduces the small-scale effects during the asynchronous modes of vibration. In this paper paper they considered the Winkler model for simulation of elastic medium between two nanoplates. In this simplified model, a proportional interaction between pressure and deflection of single layer graphene sheets (SLGSs) is assumed, which is carried out in the form of discrete and independent vertical springs. Whereas, Pasternak suggested considering not only the normal stresses but also the transverse shear deformation and continuity among the spring elements, and its subsequent applications for developing the model for buckling analysis, which proved to be more accurate than the Winkler model. Recently, analysis of the coupled system of double-layered graphene sheets (CS-DLGSs) embedded in a visco-Pasternak foundation is carried out by Ghorbanpour Arani et al. (2012a) who showed that the frequency ratio of the CS-DLGSs is more than the SLGS. Electro-thermo nonlinear vibration of a piezo-polymeric rectangular micro plate made from polyvinylidene fluoride (PVDF) reinforced by zigzag double walled boron nitride nanotubes (DWBNNTs) was studied by Ghorbanpour Arani *et al.* (2012b). Dodds (2013) studied Piezoelectric nanocomposite sensors assembled using zinc oxide nanoparticles and poly vinylidene fluoride. Numerical analysis of large amplitude free vibration behaviour of laminated composite spherical shell panel embedded with the piezoelectric layer was presented by Singh and Panda (2015). Ghorbanpour Arani *et al.* (2015a) studied nonlinear vibration and instability analysis of a bonded double-smart composite microplate system (DSCMPS) conveying microflow based on nonlocal piezoelasticity theory.Control and analyze the electro-magneto nonlinear dynamic stability of smart sandwich nano-plates were presented by Ghorbanpour Arani *et al.* (2015b). Kolahchi *et al.* (2016a) investigated nonlinear dynamic stability analysis of embedded temperature-dependent viscoelastic plates reinforced SWCNTs. Nonlinear buckling of straight concrete columns armed with SWCNTs resting on foundation was investigated by Jafarian Arani and Kolahchi (2016b). Mosharrafian and Kolahchi (2016c) presented the nanotechnology, smartness and orthotropic nonhomogeneous elastic medium effects on the buckling of piezoelectric pipes.

In this study, nonlinear transverse vibration of an embedded piezoelectric plate reinforced with SWCNTs is investigated. Considering the nonlinear strain-displacement relations and charge equation, the nonlinear governing equations are derived using energy method and Hamilton's principle. Hence, the DQM is presented to solve the nonlinear governing equations and estimate the frequency ratio of clamped supported system. In present study, the influences of geometrical aspect ratio, elastic medium constants, orientation angle and volume fraction of SWCNTs in polymer have been taken into account.

2. Formulation

Based on the classical plate theory (CPT) which satisfies Kirchhoff assumption, displacement field is expressed as (Reddy 1997)

$$u(x, y, z, t) = u_0(x, y, t) - z \frac{\partial w_0}{\partial x},$$

$$v(x, y, z, t) = v_0(x, y, t) - z \frac{\partial w_0}{\partial y},$$

$$w(x, y, z, t) = w_0(x, y, t),$$

(1)

where (u, v, w) denote the total displacements of a point along the (x, y, z) coordinates and (u_0, v_0, w_0) are the displacements of points on the mid-plane. The von Kármán nonlinear strains associated with the above displacement field can be expressed in the following form

$$\varepsilon_{xx} = \frac{\partial u}{\partial x} + \frac{1}{2}(\frac{\partial w}{\partial x})^2, \quad \varepsilon_{yy} = \frac{\partial v}{\partial y} + \frac{1}{2}(\frac{\partial w}{\partial y})^2, \quad \varepsilon_{xz} = \frac{1}{2}(\frac{\partial u}{\partial z} + \frac{\partial w}{\partial x}),$$

$$\varepsilon_{yz} = \frac{1}{2}(\frac{\partial v}{\partial z} + \frac{\partial w}{\partial y}), \quad \varepsilon_{xy} = \frac{1}{2}(\frac{\partial u}{\partial y} + \frac{\partial v}{\partial x} + \frac{\partial w}{\partial x}\frac{\partial w}{\partial y}), \quad \varepsilon_{zz} = \frac{\partial w}{\partial z},$$

(2)

On the basis of the CPT, shear strains $\varepsilon_{xz}, \varepsilon_{yz}$ are considered negligible. Hence, the strain equations in terms of the mid-plane displacements are derived by substituting the Eq. (1) into the Eq. (2) as follows

$$\begin{Bmatrix} \varepsilon_{xx} \\ \varepsilon_{yy} \\ \gamma_{xy} \end{Bmatrix} = \begin{Bmatrix} \dfrac{\partial u_0}{\partial x} + \dfrac{1}{2}(\dfrac{\partial w_0}{\partial x})^2 \\ \dfrac{\partial v_0}{\partial y} + \dfrac{1}{2}(\dfrac{\partial w_0}{\partial y})^2 \\ \dfrac{\partial u_0}{\partial y} + \dfrac{\partial v_0}{\partial y} + \dfrac{\partial w_0}{\partial x}\dfrac{\partial w_0}{\partial y} \end{Bmatrix} + z \begin{Bmatrix} -\dfrac{\partial^2 w_0}{\partial x^2} \\ -\dfrac{\partial^2 w_0}{\partial y^2} \\ -2\dfrac{\partial^2 w_0}{\partial x \partial y} \end{Bmatrix},$$

(3)

The strain components ε_{xx}, ε_{yy} and γ_{xy} at an arbitrary point of the sheet are related to the middle surface strains and curvatures tensor as follows

$$\begin{Bmatrix} \varepsilon_{xx} \\ \varepsilon_{yy} \\ \gamma_{xy} \end{Bmatrix} = \begin{Bmatrix} \varepsilon_{xx}^0 \\ \varepsilon_{yy}^0 \\ \gamma_{xy}^0 \end{Bmatrix} + z \begin{Bmatrix} \varepsilon_{xx}^1 \\ \varepsilon_{yy}^1 \\ \gamma_{xy}^1 \end{Bmatrix},$$

(4)

where $(\varepsilon_{xx}^0, \varepsilon_{yy}^0, \gamma_{xy}^0)$ are components of the membrane strains (middle surface strains) tensor and

$(\varepsilon_{xx}^{1}, \varepsilon_{yy}^{1}, \gamma_{xy}^{1})$ are components of the bending strain (curvature) tensor.

2.1 Modeling of the problem

N embedded piezoelectric plate reinforced with SWCNTs with the length L, the width b and the thickness h, assuming that $h << l, b$ (Vinson 2005), is shown in Fig. 1. The origin of the Cartesian coordinate system is considered at one corner of the middle surface of the microplate. The x, y and z axes are taken along the length, width, and thickness of the plate, respectively. The elastic medium is simulated by the Pasternak foundation.

2.2 Constitutive equations for piezoelectric materials

In a piezoelectric material, application of an electric field to it will cause a strain proportional to the mechanical field strength, and vice versa. According to a piezoelectric microplate under electro-thermal loads, constitutive equations can be represented as (Ghorbanpour Arani *et al.* 2012)

$$\begin{bmatrix} \sigma_{xx}^{nl} \\ \sigma_{yy}^{nl} \\ \sigma_{xy}^{nl} \end{bmatrix} = \begin{bmatrix} \overline{C}_{11} & \overline{C}_{12} & 0 \\ \overline{C}_{21} & \overline{C}_{22} & 0 \\ 0 & 0 & \overline{C}_{66} \end{bmatrix} \left(\begin{Bmatrix} \varepsilon_{xx} \\ \varepsilon_{yy} \\ \gamma_{xy} \end{Bmatrix} \right) - \begin{bmatrix} e_{11} & 0 & 0 \\ e_{12} & 0 & 0 \\ 0 & e_{26} & 0 \end{bmatrix} \begin{Bmatrix} E_{xx} \\ E_{yy} \\ E_{zz} \end{Bmatrix},$$

(5)

$$\begin{bmatrix} D_{xx}^{nl} \\ D_{yy}^{nl} \\ D_{xy}^{nl} \end{bmatrix} = \begin{bmatrix} e_{11} & e_{12} & 0 \\ 0 & 0 & e_{26} \\ 0 & 0 & 0 \end{bmatrix} \left(\begin{Bmatrix} \varepsilon_{xx} \\ \varepsilon_{yy} \\ \gamma_{xy} \end{Bmatrix} \right) - \begin{bmatrix} \in_{11} & 0 & 0 \\ 0 & \in_{22} & 0 \\ 0 & 0 & \in_{22} \end{bmatrix} \begin{Bmatrix} E_{xx} \\ E_{yy} \\ E_{zz} \end{Bmatrix},$$
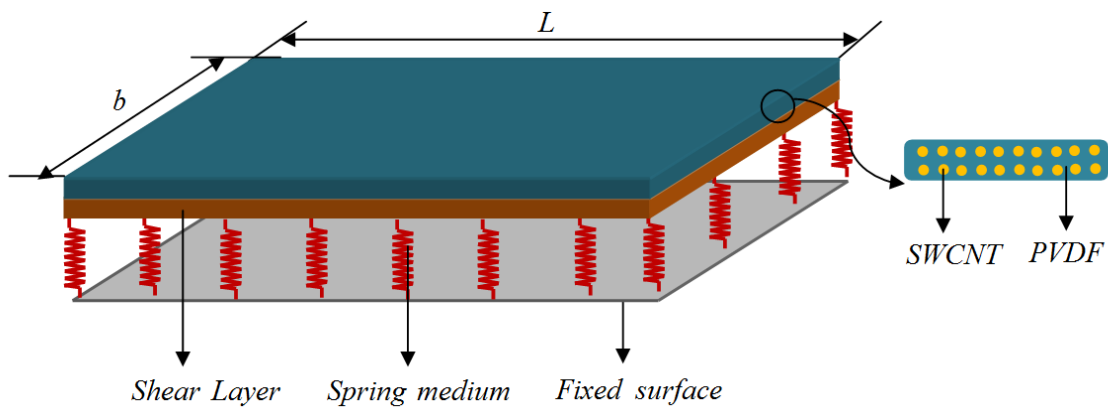
(6)

Fig. 1 Schematic of embedded piezoelectric nano-composite plate

where $e_{ij}, \in_{ij} (i, j = 1,...,6), \alpha_k (k = x, y)$ and ΔT are piezoelectric constants, dielectric constants, thermal expansion coefficients and temperature gradient, respectively. $\overline{C}_{ij}$ denote transformed stiffness components and is defined as (Reddy 1997)

$$\overline{C}_{11} = C_{11} \cos^4 \theta + 2(C_{12} + 2C_{66}) \cos^2 \theta \sin^2 \theta + C_{22} \sin^4 \theta,$$
$$\overline{C}_{12} = C_{12}(\cos^4 \theta + \sin^4 \theta) + (C_{11} + C_{22} - 4C_{66}) \cos^2 \theta \sin^2 \theta,$$
$$\overline{C}_{22} = C_{22} \cos^4 \theta + 2(C_{12} + 2C_{66}) \cos^2 \theta \sin^2 \theta + C_{11} \sin^4 \theta,$$
$$\overline{C}_{66} = (C_{11} + C_{22} - 2C_{12} - 2C_{66}) \sin^2 \theta \cos^2 \theta + C_{66}(\sin^4 \theta + \cos^4 \theta),$$

(7)

where C_{ij} are components of stiffness tensor. θ is the orientation angle between the global and local Cartesian coordinates, corresponding to the angle between SWCNTs and the main axis of the matrix. Electric field tensor E can be written in term of electric potential ϕ as (Ghorbanpour Arani *et al*. 2012)

$$E = -\nabla \phi.$$

(8)

Using approach adopted by Tan and Tong (2001) in which they use representative volume element (RVE) based on micro-electro-mechanical models, the mechanical and electrical properties of the system can be obtained.

2.3 Equations of motion

The governing differential equations of motion are derived using the Hamilton's principle which is given as

$$\int_0^T (\delta U + \delta V - \delta K) dt = 0$$

(9)

where δU is the virtual strain energy, δV is the virtual work done by external applied forces and δK is the virtual kinetic energy. The motion equations can be derived using Eq. (9) as follows

$$\frac{\partial N_{xx}}{\partial x} + \frac{\partial N_{xy}}{\partial y} = m_0 \frac{\partial^2 u_0}{\partial t^2},$$

$$\frac{\partial N_{xy}}{\partial x} + \frac{\partial N_{yy}}{\partial y} = m_0 \frac{\partial^2 v_0}{\partial t^2},$$

$$\frac{\partial^2 M_{xx}}{\partial x^2} + 2\frac{\partial^2 M_{xy}}{\partial y \partial x} + \frac{\partial^2 M_{yy}}{\partial y^2} + \frac{\partial}{\partial x}(N_{xx}\frac{\partial w_0}{\partial x} + N_{xy}\frac{\partial w_0}{\partial y}) + \frac{\partial}{\partial y}(N_{xy}\frac{\partial w_0}{\partial x} + N_{yy}\frac{\partial w_0}{\partial y})$$

$$- K_W w_0 + K_G (\frac{\partial^2 w_0}{\partial x^2} + \frac{\partial^2 w_0}{\partial y^2}) + q = m_0 \frac{\partial^2 w_0}{\partial t^2} - m_2 \frac{\partial^2}{\partial t^2}(\frac{\partial^2 w_0}{\partial x^2} + \frac{\partial^2 w_0}{\partial y^2}),$$

(10)

where

$$(m_0, m_2) = \int_{-h/2}^{h/2} \rho_0 (1, z^2) dz \tag{11}$$

where (m_0, m_2) are mass moments of inertia and ρ_0 denotes the density of the material. Meanwhile, the force resultants (N_{xx}, N_{yy}, N_{xy}) and the moment resultants (M_{xx}, M_{yy}, M_{xy}) of plate can be defined as

$$\{(N_x, N_y, N_{xy}), (M_x, M_y, M_{xy})\} = \int_{-h/2}^{h/2} \{\sigma_x, \sigma_y, \tau_{xy}\}(1, z) dz \tag{12}$$

Charge equation for coupling electrical and mechanical fields is

$$\frac{\partial D_x}{\partial x} + \frac{\partial D_y}{\partial y} + \frac{\partial D_z}{\partial z} = 0, \tag{13}$$

In this study, transverse vibration is investigated (i.e. $u_0 = v_0 = 0$). Considering $w_0(x, y, t) = W(x, y)e^{i\omega t}$ and defining dimensionless parameters as follows

$$\beta_x = \frac{h}{l}, \quad \beta_y = \frac{h}{b}, \quad Q_1 = \frac{\overline{C}_{12}}{\overline{C}_{11}}, \quad Q_2 = \frac{\overline{C}_{22}}{\overline{C}_{11}}, \quad Q_3 = \frac{\overline{C}_{66}}{\overline{C}_{11}}, \quad T_x = \alpha_{xx}T,$$

$$T_y = \alpha_{yy}T, \quad K_G^* = \frac{k_g}{\overline{C}_{11}l}, \quad K_W^* = \frac{k_w l}{\overline{C}_{11}}, \quad \overline{m}_0 = \frac{m_0}{\rho_0 l}, \quad \overline{m}_2 = \frac{m_2}{\rho_0 l^3},$$

$$\Omega = \omega l \sqrt{\frac{\rho_0}{\overline{C}_{11}}}, \quad \phi_0 = l \sqrt{\frac{\overline{C}_{11}}{\epsilon_{11}}}, \quad \overline{e}_1 = \frac{e_{11} \phi_0}{\overline{C}_{11}l} = \frac{e_{11}}{\sqrt{\overline{C}_{11} \epsilon_{11}}},$$

$$\overline{e}_2 = \frac{e_{12} \phi_0}{\overline{C}_{11}l} = \frac{e_{12}}{\sqrt{\overline{C}_{11} \epsilon_{11}}}, \quad \overline{e}_3 = \frac{e_{26} \phi_0}{\overline{C}_{11}l} = \frac{e_{26}}{\sqrt{\overline{C}_{11} \epsilon_{11}}}, \quad \mu^* = \frac{\mu}{l^2},$$

$$\zeta = \frac{x}{l}, \quad \eta = \frac{y}{b}, \quad W^* = \frac{W}{h}, \quad \Phi = \frac{\phi}{\phi_0}, \tag{14}$$

As well as substituting combination of Eqs. (1)-(5) and (12) into Eqs. (10) and (13) the dimensionless nonlinear transverse nonlocal motion equations of DPCMPS can be written as

$$\frac{-1}{12} \beta_x^4 \frac{\partial^4 W^*}{\partial \zeta^4} - \frac{1}{6} \beta_x^2 \beta_y^2 (Q_1 + 2Q_3) \frac{\partial^4 W^*}{\partial \eta^2 \partial \zeta^2} - \frac{1}{12} Q_2 \beta_y^4 \frac{\partial^4 W^*}{\partial \eta^4} - + \beta_x^2 \overline{e}_1 \frac{\partial^2 W^*}{\partial \zeta^2} \frac{d\Phi}{d\zeta} +$$

$$\beta_y^2 \overline{e}_2 \frac{\partial^2 W^*}{\partial \eta^2} \frac{d\Phi}{d\eta} + \Omega^2 \left[\overline{m}_0 \beta_x W_{(m)}^* - \overline{m}_2 (\beta_x \frac{\partial^2 W^*}{\partial \zeta^2} + \frac{\beta_y^2}{\beta_x} \frac{\partial^2 W^*}{\partial \eta^2}) \right]$$

$$- K_W^* \beta_x W^* + K_G^* \left(\beta_x (\frac{\partial^2 W^*}{\partial \zeta^2}) + \frac{\beta_y^2}{\beta_x} (\frac{\partial^2 W^*}{\partial \eta^2}) \right) = 0, \tag{15}$$

$$\beta_x^4 \bar{e}_1 (\frac{\partial W^*}{\partial \zeta} \frac{\partial^2 W^*}{\partial \zeta^2}) + \bar{e}_2 \beta_x^2 \beta_y^2 (\frac{\partial W^*}{\partial \eta} \frac{\partial^2 W^*}{\partial \eta \partial \zeta}) + \bar{e}_3 \beta_x^2 \beta_y^2 (\frac{\partial W^*}{\partial \eta} \frac{\partial^2 W^*}{\partial \eta \partial \zeta} +$$

$$\frac{\partial W^*}{\partial \zeta} \frac{\partial^2 W^*}{\partial \eta^2}) - \beta_x^2 \frac{d^2 \Phi}{d \zeta^2} = 0,$$

(16)

The clamped supported mechanical and free electrical boundary conditions can be expressed as

$$W^* = \Phi = 0, \ \partial W^* / \partial \zeta = 0 \ \text{at edges} \ \zeta = 0 \ \text{and} \ \zeta = 1$$

$$W^* = \Phi = 0, \ \partial W^* / \partial \zeta = 0 \ \text{at edges} \ \eta = 0 \ \text{and} \ \eta = 1$$

(17)

2.4 DQ method

As can be seen the coupled governing equations contain nonlinear terms and should be solved using a numerical method such as DQM. In this method, the differential equations are changed into a first order algebraic equation by employing appropriate weighting coefficients. Weighting coefficients do not relate to any special problem and only depend on the grid spacing. For implementation of the DQ approximation, consider a function $f(\zeta, \eta)$ which has the field on a rectangular domain ($0 \le \zeta \le 1$ and $0 \le \eta \le 1$) with $n_\zeta \times n_\eta$ grid points along x and y axes. According to DQ method, the rth derivative of a function $f(x, y)$ can be defined as (Kolahchi *et al.* 2015)

$$\frac{\partial^r f(\zeta, \eta)}{\partial \zeta^r}\bigg|_{(\zeta, \eta) = (\zeta_i, \eta_j)} = \sum_{m=1}^{n_\zeta} C_{im}^{\zeta(r)} f(\zeta_m, \eta_j) = \sum_{m=1}^{n_x} C_{im}^{\zeta(r)} f_{mj}, \quad \begin{cases} i = 1, 2, ..., n_\zeta \\ j = 1, 2, ..., n_\eta \\ r = 1, 2, ..., n_\zeta - 1 \end{cases}$$

(18)

where C_{ij}^{ζ} are weighting coefficients and defined as

$$C_{ij}^{\zeta} = \begin{cases} \dfrac{M(\zeta_i)}{(\zeta_i - \zeta_j) M(\zeta_j)} & \text{for} \ i \ne j \\ -\displaystyle\sum_{\substack{j=1 \\ i \ne j}}^{n_\zeta} C_{ij}^{\zeta} & \text{for} \ i = j \end{cases},$$

(19)

where $M(\zeta_i)$ is Lagrangian operators which can be presented as

$$M(\zeta_i) = \prod_{\substack{j=1 \\ i \ne j}}^{n_\zeta} (\zeta_i - \zeta_j).$$

(20)

The weighting coefficients for the second, third and fourth derivatives are defined as

$$C_{ij}^{\zeta(2)} = \sum_{k=1}^{n_\zeta} C_{ik}^{\zeta(1)} C_{kj}^{\zeta(1)}, \quad C_{ij}^{\zeta(3)} = \sum_{k=1}^{n_\zeta} C_{ik}^{\zeta(1)} C_{kj}^{\zeta(2)} = \sum_{k=1}^{n_\zeta} C_{ik}^{\zeta(2)} C_{kj}^{\zeta(1)}$$

$$C_{ij}^{\zeta(4)} = \sum_{k=1}^{n_\zeta} C_{ik}^{\zeta(1)} C_{kj}^{\zeta(3)} = \sum_{k=1}^{n_\zeta} C_{ik}^{\zeta(3)} C_{kj}^{\zeta(1)}.$$

(21)

In a similar method, the weighting coefficients for y-direction can be obtained. The coordinates of grid points are chosen as

$$\zeta_i = \frac{1}{2}\left[1 - \cos(\frac{\pi(i-1)}{(n_x-1)})\right], \eta_j = \frac{1}{2}\left[1 - \cos(\frac{\pi(j-1)}{(n_y-1)})\right].$$

(22)

The motion equations using DQM can be rewritten as

$$-\frac{1}{12}\beta_x^4(\sum_{k=1}^{n_x} C_{i,k}^{\zeta(4)} W_{k,j}^*) - \frac{1}{6}\beta_x^2\beta_y^2(Q_1 + 2Q_3)(\sum_{k_1=1}^{n_x}\sum_{k_2=1}^{n_y} C_{i,k_1}^{\zeta(2)} C_{j,k_2}^{\eta(2)} W_{k_1,k_2}^*) - \frac{1}{12}Q_2\beta_y^4(\sum_{k=1}^{n_y} C_{j,k}^{\eta(4)} W_{i,k}^*)$$

$$+ \beta_x^2\bar{e}_1(\sum_{k=1}^{n_x} C_{i,k}^{\zeta(2)} W_{k,j}^*)(\sum_{k=1}^{n_x} C_{i,k}^{\zeta(1)} \Phi_{k,j}) + \beta_y^2\bar{e}_2(\sum_{k=1}^{n_x} C_{j,k}^{\eta(2)} W_{i,k}^*)(\sum_{k=1}^{n_x} C_{i,k}^{\zeta(1)} \Phi_{k,j})$$

$$+ \Omega^2\left[\bar{m}_0\beta_x W_{i,j}^* - \bar{m}_2(\beta_x(\sum_{k=1}^{n_x} C_{i,k}^{\zeta(2)} W_{k,j}^*) + \frac{\beta_y^2}{\beta_x}(\sum_{k=1}^{n_y} C_{j,k}^{\eta(2)} W_{i,k}^*))\right] - K_W^*\beta_x(W_{i,j}^*)$$

$$+ K_G^*(\beta_x(\sum_{k=1}^{n_x} C_{i,k}^{\zeta(2)} W_{k,j}^*) + \frac{\beta_y^2}{\beta_x}(\sum_{k=1}^{n_y} C_{j,k}^{\eta(2)} W_{i,k}^*) = 0$$

(23)

$$\beta_x^4\bar{e}_1((\sum_{k=1}^{n_x} C_{i,k}^{\zeta(1)} W_{k,j}^*)(\sum_{k=1}^{n_x} C_{i,k}^{\zeta(2)} W_{k,j}^*)) + \bar{e}_2\beta_x^2\beta_y^2((\sum_{k=1}^{n_y} C_{j,k}^{\eta(1)} W_{i,k}^*)(\sum_{k_1=1}^{n_x}\sum_{k=1}^{n_y} C_{i,k_1}^{\zeta(1)} C_{j,k_2}^{\eta(1)} W_{k_1,k_2}^*))$$

$$+ \bar{e}_3\beta_x^2\beta_y^2((\sum_{k=1}^{n_y} C_{j,k}^{\eta(1)} W_{i,k}^*)(\sum_{k_1=1}^{n_x}\sum_{k=1}^{n_y} C_{i,k_1}^{\zeta(1)} C_{j,k_2}^{\eta(1)} W_{k_1,k_2}^*) + (\sum_{k=1}^{n_x} C_{i,k}^{\zeta(1)} W_{k,j}^*)(\sum_{k=1}^{n_y} C_{j,k}^{\eta(4)} W_{i,k}^*))$$

$$+ \beta_x^2(\sum_{k=1}^{n_x} C_{i,k}^{\zeta(2)} \Phi_{k,j}) = 0$$

(24)

In order to carry out the eigenvalue analysis, the domain and boundary points are separated and in vector forms they are denoted as {d} and {b}, respectively. Hence, the discretized form of the motion equations together with the boundary conditions can be expressed in matrix form as

$$\left(\underbrace{[K_L + K_{NL}]}_{[K]} - \Omega^2[M]\right)\begin{bmatrix}\{d\}\\\{b\}\end{bmatrix} = 0,$$

(25)

in which $[M]$, $[K_L]$ and $[K_{NL}]$ are the mass matrix, linear stiffness matrix and nonlinear stiffness matrix. This nonlinear equation can now be solved using a direct iterative process as follows

- First, nonlinearity is ignored by taking $[K_{NL}]=0$ to solve the eigenvalue problem expressed in Eq. (25). This yields the linear eigenvalue (Ω_L) and associated eigenvector. The eigenvector is then scaled up so that the maximum transverse displacement of the microplate is equal to the maximum eigenvector, i.e. the given vibration amplitude $W_{\max}^*$.

- Using linear eigenvector, $[K_{NL}]$ could be evaluated. Eigenvalue problem is then solved by substituting $[K_{NL}]$ into Eq. (25). This would give the nonlinear eigenvalue (Ω_{NL}) and the new eigenvector.

The new nonlinear eigenvector is scaled up again and the above procedure is repeated iteratively until the frequency values from the two subsequent iterations ' r ' and ' $r+1$ ' satisfy the prescribed convergence criteria as

$$\frac{\left|\omega^{r+1}-\omega^r\right|}{\omega^r}<\varepsilon_0$$

(32)

where ε_0 is a small value number and in the present analysis it is taken to be 0.1% .

3. Numerical results and discussion

Mechanical, thermal and electrical properties of PVDF matrix and SWCNTs reinforcement are taken from Ref. (Lei *et al.* 2012). The final converged solution using the numerical procedure outlined in Section 2.6 above is illustrated as the influences of the elastic medium, aspect ratio, orientation angle of SWCNTs in polymer and volume percent of SWCNTs in and on the frequency ratio of the system. The frequency ratio is defined as

$$\text{Frequency Ratio} = \frac{\Omega_{NL}}{\Omega_L},$$

where Ω_{NL} and Ω_L are the nonlinear and linear frequencies of the system, respectively.

In order to show the effect of dimensionless elastic medium constants, the frequency ratio (Ω_{NL}/Ω_L) versus the dimensionless maximum amplitude ($W_{\max}^*$) is demonstrated in Figs. 2 and 3. Noted that the elastic medium in this study is simulated as spring constants of Winkler-type (K_W^*) and shear constants of Pasternak-type (K_G^*). In general, the frequency ratio decreases with increasing elastic medium constants. This is because increasing Winkler and Pasternak coefficients increases the system stiffness. Furthermore, the effect of Pasternak medium is higher that Winkler one. It is due to the fact that Pasternak foundation considers normal and shear loads.

The effect of geometrical aspect ratio (β_x) on the frequency ratio versus the dimensionless maximum amplitude is shown in Fig. 4. It is clear that the Ω_{NL}/Ω_L increases with increasing the $W_{\max}^*$ and the influence of geometrical aspect ratio becomes more prominent at the higher dimensionless maximum amplitude. It is also found that the Ω_{NL}/Ω_L is decreased with increasing the β_x, since the equivalent stiffness of the system increases.
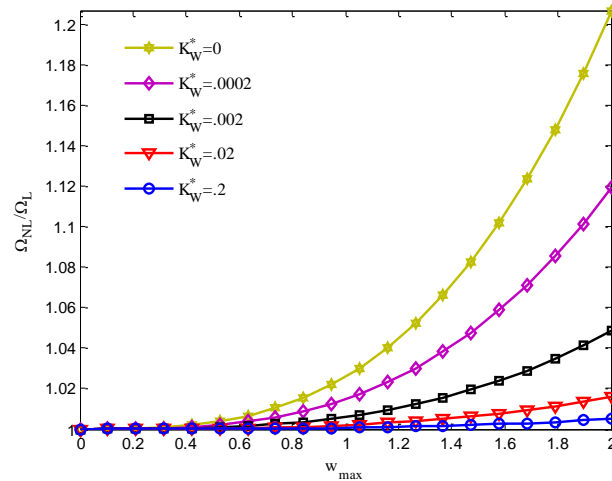
Fig. 2 The effect of spring constant of elastic medium on the frequency ratio versus the dimensionless maximum amplitude
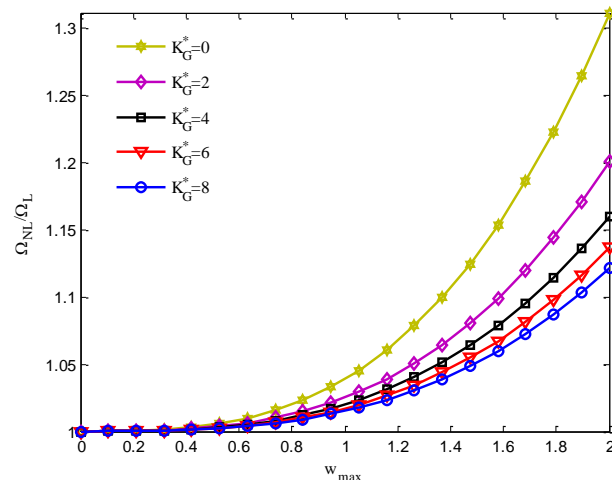

Fig. 3 The effect of shear constant of elastic medium on the frequency ratio versus the dimensionless maximum amplitude

In realizing the influence of SWCNT volume percent (ρ) in polymer, Fig. 5 indicates how frequency ratio changes with respect to the dimensionless maximum amplitude. Generally, the frequency ratio of the system is decreased with increasing ρ. This is why, the Yong's modulus of reinforcer (e.g., SWCNT) is much greater than polymer (e.g., PVDF). Therefore, with increasing ρ, elastic constants of the composite increase and consequently the piezoelectric composite plates become more stable.
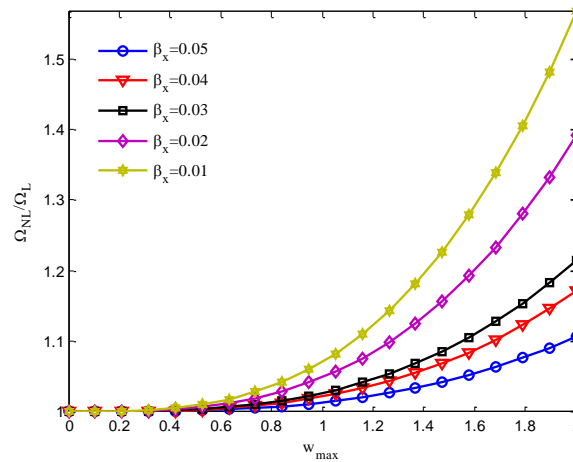
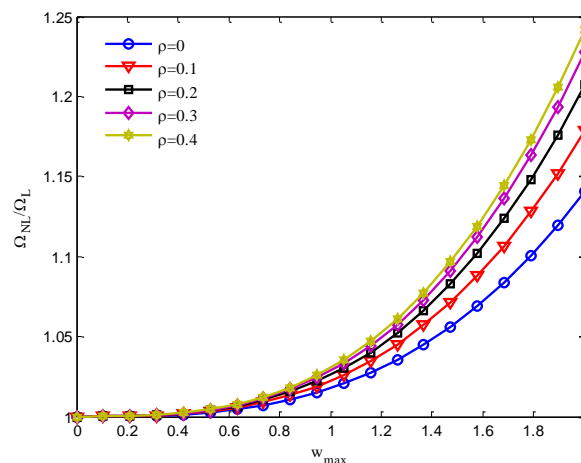Fig. 4 The effect of aspect ratio on the frequency ratio versus the dimensionless maximum amplitude

Fig. 5 The effect of SWCNT volume percent in polymer on the frequency ratio versus the dimensionless maximum amplitude

Fig. 6 demonstrates variations of the frequency ratio versus the dimensionless maximum amplitude. Noted that Fig. 5 is plotted for different values of SWCNT orientation angle in polymer which are taken as $\theta = 0$, $\theta = \pi/6$, $\theta = \pi/4$, $\theta = \pi/3$ and $\theta = \pi/2$, respectively. As can be seen Ω_{NL}/Ω_L is significantly dependent on θ so that the frequency ratio increases with increasing orientation angle. Moreover, frequency ratio of $\theta = \pi/2$ and $\theta = 0$ are maximum and minimum, respectively. This is most likely due to the fact that in $\theta = 0$, the direction of polarization for both reinforcements (SWCNT) and matrix (PVDF) are the same which makes the system stiffer and leads to increase in frequency and consequently, decrease in frequency ratio.
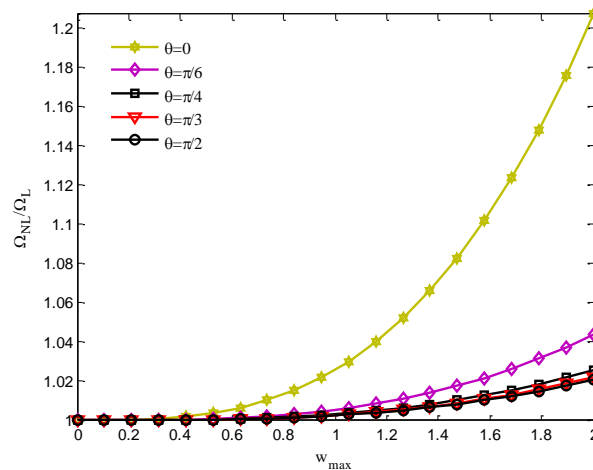
Fig. 6 The effect of SWCNT orientation angle in polymer on the frequency ratio versus the dimensionless maximum amplitude
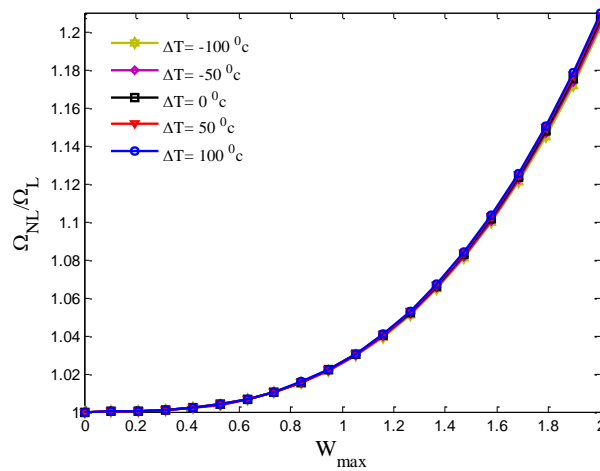

Fig. 7 The effect of temperature change on the frequency ratio versus the dimensionless maximum amplitude

Fig. 7 illustrates the influence of thermal gradient (ΔT) on the frequency ratio versus the dimensionless maximum amplitude. It is evident that an increase in temperature change does not affect on the frequency ratio.

4. Conclusions

Vibration response of piezoelectric composites has applications in designing many NEMS/MEMS devices such as hydraulic sensors and actuators. In the present study, nonlinear

vibration of a piezoelectric nano-composite plate made of PVDF reinforced by SWCNT is investigated. The surrounding elastic medium is simulated as Pasternak foundation. Considering charge equation, the nonlinear motion equations are derived based on energy method. The DQM is applied to obtain to the nonlinear frequency ratio of the system so that the effects of the stiffness of the elastic medium, the volume fraction, orientation angle of the SWCNTs reinforcement, temperature change and aspect ratio are discussed. The results indicate that with increasing geometrical aspect ratio, the frequency ratio decreases. Furthermore, frequency ratio of $\theta = \pi / 2$ and $\theta = 0$ are maximum and minimum, respectively. In addition, the frequency ratio of the system is decreased with increasing SWCNT volume percent.

Acknowledgments

References

Antonio Arnau, V. (2008), *Piezoelectric Transducers and Applications*, Heidelberg: Springer-Verlag Berlin.

Chen, W.Q., Bian, Z.G., Lv, C.F. and Ding, H.J. (2004), "3D free vibration analysis of a functionally graded piezoelectric hollow cylinder filled with compressible fluid", *Int. J. Solids Struct.*, **41**(3-4), 947-964.

Dodds, J.S., Meyers F.N. and Loh, K.J. (2013), "Piezoelectric nanocomposite sensors assembled using zinc oxide nanoparticles and poly(vinylidene fluoride)", *Smart Struct. Syst.*, **12**(1), 55-71.

Ghorbanpour Arani, A., Shiravand, A., Rahi, M. and Kolahchi, R. (2012a), "Nonlocal vibration of coupled DLGS systems embedded on Visco-Pasternak foundation", *Physica B*, **407**(21), 4123-4131.

Ghorbanpour Arani, A., Vossough, H., Kolahchi, R. and Mosallaie Barzoki, A.A. (2012b), "Electro-thermo nonlocal nonlinear vibration in an embedded polymeric piezoelectric micro plate reinforced by DWBNNTs using DQM", *J. Mech. Sci. Technol.*, **26**(10), 3047-3057.

Ghorbanpour Arani, A., Vossough, H. and Kolahchi, R. (2015a), "Nonlinear vibration and instability of a visco-Pasternak coupled double-DWBNNTs-reinforced microplate system conveying microflow", *Proc. IMechE Part C: J. Mech. Eng. Sci.*, **229**, 3274-3290.

Ghorbanpour Arani, A., Kolahchi, R. and Zarei, M.Sh. (2015b), "Visco-surface-nonlocal piezoelasticity effects on nonlinear dynamic stability of graphene sheets integrated with ZnO sensors and actuators using refined zigzag theory", *Compos. Struct.*, **132**, 506-526.

Ke L.L. and Sritawat Kitipornchai, J.Y. (2011), "Dynamic stability of functionally graded carbon nanotube-reinforced composite beams", *Mech. Adv.. Mater. Struct.*, **18**, 262-271.

Kireitseu, M.V., Tomlinson, G.R., Ivanenko, A.V. and Bochkareva, L.V. (2007), "Dynamics and vibration damping behavior of advanced Meso/Nanoparticle-reinforced composites", *Mech. Adv.. Mater. Struct.*, **14**, 603-617.

Kolahchi, R., Rabani Bidgoli, M., Beygipoor, Gh. and Fakhar, M.H. (2015), "A nonlocal nonlinear analysis for buckling in embedded FG-SWCNT-reinforced microplates subjected to magnetic field", *J. Mech. Sci. Technol.*, **29**(9), 3669-3677.

Kolahchi, R., Safari, M. and Esmailpour, M. (2016a), "Dynamic stability analysis of temperature-dependent functionally graded CNT-reinforced visco-plates resting on orthotropic elastomeric medium", *Compos. Struct.*, **150**, 255-265.

Jafarian Arani, A. and Kolahchi, R. (2016b), "Buckling analysis of embedded concrete columns armed with

carbon nanotubes", *Comput. Concre.*, **17**(5), 567-578.

Mosharrafian, F. and Kolahchi, R. (2016c), "Nanotechnology, smartness and orthotropic nonhomogeneous elastic medium effects on buckling of piezoelectric pipes", *Struct. Eng. Mech.*, **58**(5), 931-947.

Kotsilkova, R. (2007), *Thermoset Nanocomposites for Engineering Applications*, Smithers Rapra Technology, UK.

Lei, X.W., Natsuki, T., Shi, J.X. and Ni, Q.Q. (2012), "Surface effects on the vibrational frequency of double-walled carbon nanotubes using the nonlocal Timoshenko beam model", *Compos. Part B*, **43**(1), 64-69.

Murmu, T. and Adhikari, S. (2011), "Nonlocal vibration of bonded double-nanoplate-systems", *Compos. Part B*, **42**(7), 1901-1911.

Reddy, J.N. (1997), *Mechanics of Laminated Composite Plates*, Theory and Analysis, Boca Raton, Chemical Rubber Company.

Singh V.K. and Panda S.K. (2015), "Large amplitude free vibration analysis of laminated composite spherical shells embedded with piezoelectric layers", *Smart Struct. Syst.*, **16**(5), 853-872.

Tan, P. and Tong, L. (2001), "Micro-electromechanics models for piezoelectric-fiber-reinforced composite materials", *Compos. Sci. Technol.*, **61**(5), 759-769.

Vinson, J.R. (2005), *Plate and panel structures of isotropic, composite and piezoelectric materials, including sandwich construction*, Springer, USA.

CC